PRAMANA
— journal of
physics

Vol. 61, No. 4
October 2003
pp. 675–684

Quantum molecular dynamics approach to estimate spallation yield from p + ^{208}Pb reaction at 800 MeV

P K SARKAR[1,*] and MAITREYEE NANDY[2]
[1]H.P. Unit, Variable Energy Cyclotron Centre, 1/AF, Bidhan Nagar, Kolkata 700 064, India
[2]Saha Institute of Nuclear Physics, 1/AF, Bidhan Nagar, Kolkata 700 064, India
[*]Corresponding author
Email: pks@veccal.ernet.in

MS received 21 October 2002; revised 24 April 2003; accepted 21 May 2003

Abstract. The spallation yield of neutrons and other mass fragments produced in 800 MeV proton induced reaction on ^{208}Pb have been calculated in the framework of quantum molecular dynamics (QMD) model. The energy spectra and angular distribution have been calculated. Also, multiplicity distributions of the emitted neutrons and kinetic energy carried away by them have been estimated and compared with the available experimental data. The agreement is satisfactory. A major contribution to the neutron emission comes from statistical decay of the fragments. For mass and charge distributions of spallation products the QMD process gives rise to target-like and projectile-like fragments only.

Keywords. Spallation reaction; neutron emission; spallation products; quantum molecular dynamics.

PACS Nos 25.40.Sc; 25.40.-h; 28.20.-v

1. Introduction

In recent years, spallation neutron sources are used extensively for material science studies. Additionally, they provide an important link between the accelerator and the subcritical multiplying system in proposed accelerator driven technologies for production of energy and transmutation of long-lived wastes in a, possibly, cleaner and safer way. Consequently, the need for reliable data to design and construct spallation neutron sources has prompted renewed interest in the corresponding nuclear data. Some such information are too difficult, expensive and even inaccessible by measurement and therefore, are required to be estimated theoretically. To do so we require an insight into the physics of the spallation reaction mechanism, the initial non-equilibrium process which leads to the formation of excited nuclei (fragments) subsequently decaying by evaporating (predominantly) light particles like neutrons, ^{1}H, ^{2}H, ^{3}H, ^{3}He and ^{4}He.

Amongst the spallation products, gaseous elements like hydrogen, helium etc has strong bearings on the structural damages caused to the target material and the beam window.

Production of radioactive gases like tritium and other long-lived radiotoxic elements may require special radiation safety provisions.

An important quantity in the design of a spallation source is the neutron cost, which involves the neutron yield and the running cost of the accelerator. This cost is inversely proportional to the number of emitted neutrons normalized to the unit beam energy per incident particle. This cost is found to be minimum around 1 GeV of proton energy [1]. The energy and angular distributions of the spallation produced neutrons for model probing and for optimizing the target geometry are also important.

Intra-nuclear cascade (INC) models together with sequential statistical evaporation models are generally used to calculate spallation yields of neutrons and light ions. The INC models take care of the initial high energy part of the reaction process. The scattering and decay of all the produced hadrons are followed until they leave the composite nucleus or thermal equilibrium is reached when the nucleus decays further via sequential statistical evaporation. However, the transition from fast INC to the statistical decay of an equilibrated compound nucleus cannot be abrupt. For a smooth transition pre-equilibrium (PEQ) emissions need to be considered in between. The measured high energy component of the emission spectra of nucleons and composite particles is a clear indicator of that [2]. In the present work we have used a quantum molecular dynamics (QMD) approach followed by a statistical decay model (SDM) approach to treat spallation reactions induced in a Pb target by 800 MeV protons. The code we have used for the present work has been developed by Niita et al [3]. The QMD has certain advantages in describing the non-equilibrium reaction mechanism since both the high energy cascade and pre-equilibrium processes are combined in its unified formulations in a self-consistent way [3]. Futhermore, the QMD has a clear advantage over the INC based calculations in calculating the various mass fragments formed in the spallation reaction. In INC the fragmentation of the composite nucleons is not considered explicitly. Therefore, the QMD calculations are used to estimate the yield of radionuclides in the spallation process. The aim of the present work is to compare the QMD results with those obtained experimentally as well as from INC models. Such comparisons will provide a kind of validation of the QMD model which can be used to calculate radionuclide production. A major disadvantage of the QMD code is its inability to calculate thick target yields which is important for application. However, this problem is being solved by recent efforts to incorporate QMD in high energy transport codes. In §2 we give a brief description of the model followed by results and discussions in §3.

2. Description of the model

Spallation reactions are generally described by a two step process. In the first stage successive hard collisions between the projectile and the target nucleons lead to emission of fast particles which is followed by the decay of the excited residual nucleus by emission of low energy particles or by fission. The first stage is widely described by INC models while the evaporation-fission model is used for the second stage. There are several commonly used INC models like the old Bertini [4] or the Cugnon INC models [5]. The most widely used evaporation model to explain spallation reactions is the Dressner model [6] in conjunction with the Atchison fission model [7]. The INC models follow elastic and inelastic (excitation of the Δ-resonance) scattering of the incident or secondary hadrons inside the

nucleus. They use free hadron–nucleon cross sections for the particles to be scattered into unoccupied final states (Pauli blocking) inside the nucleus or into the continuum outside the nucleus.

Although there are a few codes based on intra nuclear cascade followed by evaporation-fission to calculate spallation yields, there exist large discrepancies between experimental data and model predictions and also between different models. This was evident after the intercomparison of the codes organized by OECD/NEA [8]. In an earlier work [9] the Bertini model was found to largely overpredict the experimental data. When PEQ mechanism is combined with the Bertini model it reproduces the experimental data well for 800 MeV proton-induced reactions on Pb but the agreement becomes worse as one goes to lighter masses or higher incident energies [2]. Some of the INC model based codes (like the recent version of LAHET) incorporate pre-equilibrium calculations as an optional plug-in feature. The study of pre-equilibrium nuclear reactions have been an active field since 1948 and many like semiclassical and quantum mechanical models have been proposed. These theories give an overall agreement with the experimental data, but still there are open questions which need further investigations for the problems to be satisfactorily resolved. Furthermore, coupling of pre-equilibrium models with INC does not appear to be congruent either and, as such, it also fails to reproduce the experimental data [10].

The QMD model simulates the heavy-ion reaction in an event-by-event basis. Collisions among the nucleons are forbidden when the final transition occurs to already occupied or partially occupied states. The nucleons are represented by Wigner densities of Gaussian wave packets of width L of the form [3]

$$f_i(\vec{r}_i,\vec{p}_i,t) = \frac{1}{\pi h^3}\exp\left(-\frac{[\vec{r}_i-\vec{r_{i0}}(t)]^2}{2L} - [\vec{p}_i-\vec{p_{i0}}(t)]^2\frac{2L}{h^2}\right). \tag{1}$$

r_{i0} and p_{i0} are the centroids of position and momentum of the ith nucleon. The distribution function for the total system is the sum of all nucleon wave packets

$$f(\vec{r},\vec{p},t) = \sum_i f_i(\vec{r}_i,\vec{p}_i,t). \tag{2}$$

The baryon density is expressed in terms of these Gaussian functions.

The time evolution of r_i and p_i is described by Newtonian equations and stochastic two-nucleon collisions

$$\dot{\vec{r}}_i = \{H,\vec{r}_i\}, \tag{3}$$

$$\dot{\vec{p}}_i = \{H,\vec{p}_i\}, \tag{4}$$

where the Hamiltonian H consists of kinetic part, Skryme, Coulomb, Yukawa interaction part and the symmetry energy. Often a two- and three-body Skyrme interaction is used. The two nucleon collision which takes into account the Pauli blocking in the final state is also introduced. The change in the relative importance of the mean field effects and two-body collisions gives a transition between equilibrium, pre-equilibrium and spallation mechanisms including fast multi-particle emissions. It has been emphasized that non-equilibrium effects play an important role in heavy-ion collisions which has been accounted for through the incorporation of momentum-dependent nuclear interaction which leads to an additional repulsion between nucleons.

The QMD theory considers among other physics aspects of the intermediate energy nuclear reactions: realistic momentum distribution of the nucleons inside the nucleus, multistep process, multiple pre-equilibrium emission process, variation of the mean field potential because of particle hole excitation and particle emission, energy-dependent anisotropic nucleon–nucleon elastic and inelastic scattering including the Pauli blocking effect.

The total hamiltonian for the system is given by

$$H = \sum_i \sqrt{m_i^2 + P_i^2} + \frac{1}{2}\frac{A}{\rho_0}\sum_i \langle\rho_i\rangle + \frac{1}{1+\tau}\frac{B}{\rho_0^\tau}\sum_i \langle\rho_i\rangle^\tau + \frac{1}{2}\sum_{i,j(\neq i)} c_i c_j \frac{e^2}{|\,\mathbf{R}_i - \mathbf{R}_j\,|}\,\mathrm{erf}(|\,\mathbf{R}_i - \mathbf{R}_j\,|/\sqrt{4L}) + \frac{C_s}{2\rho_0}\sum_{i,j(\neq i)} (1 - 2\,|\,c_i - c_j\,|)\rho_{ij}. \quad (5)$$

Here m_i is the mass of the ith nucleon. The symmetry energy coefficient C_s, the saturation density ρ_0, Skryme parameters A, B and τ are chosen to be 25 MeV, 0.168 fm^{-3}, -124 MeV, 70.5 MeV and 4/3, respectively. The width parameter L is fixed to be 2 fm^2, 'erf' denotes the error function and c_i is 1 for protons and 0 for neutrons. ρ_i and $\langle\rho_i\rangle$ are defined as

$$\rho_i(r) = \int \frac{\mathrm{d}\mathbf{p}}{(2\pi\hbar)^3} f_i(\mathbf{r},\mathbf{p}) = (2\pi L)^{-3/2}\exp\left[-(\mathbf{r}-\mathbf{R}_i)^2/2L\right] \quad (6)$$

and

$$\langle\rho_i\rangle \equiv \sum_{j(\neq i)} \rho_{ij} \equiv \sum_{j(\neq i)} \int \mathrm{d}\mathbf{r}\rho_i(\mathbf{r})\rho_j(\mathbf{r}) = \sum_{j(\neq i)} (4\pi L)^{-3/2}\exp\left[-(\mathbf{R}_i - \mathbf{R}_j)^2/4L\right]. \quad (7)$$

Time evolution of $\vec{r}_i$ and $\vec{p}_i$ are determined from eqs (3) and (4). Each particle trajectory is thus followed through the nuclear volume and once it escapes the nuclear boundary emission is considered. Cluster emission is inferred when the positions and momenta of the constituent particles lie within a previously defined range. The QMD theory is combined with a statistical decay model (SDM) to estimate evaporation from residual nuclei following fast particle emissions.

3. Results and discussions

Calculations have been performed for 800 MeV protons on ^{208}Pb and all the results shown are in the laboratory frame of reference. The QMD calculations are done for 6000 histories. The particle trajectory is followed in a time step of 1 fm/c and the maximum impact parameter is fixed at 7 fm.

We have calculated the differential neutron emission cross section $\mathrm{d}\sigma/\mathrm{d}E$ (figure 1) where we have shown separately the contributions from the QMD and the SDM processes. It is seen that the SDM process is responsible for low energy emission restricted up to about 50 MeV and accounts for the major portion (73%) of the total neutron emission. The QMD, on the other hand, gives rise to high energy neutrons with energies extending beyond 400 MeV.

The energy integrated angular distribution of the neutrons (figure 2) shows a predominant forward angle emission for the QMD process while the neutrons from the SDM calculations have more or less isotropic angular distribution with respect to the incident proton direction. Thus the double differential neutron emission cross-section (or multiplicity) at various angles will differ only in the high energy component (contributed by the QMD process) with a decrease in the emission for larger angles. This theoretical inference is in conformity with the experimental results of Leray *et al* [2].

The energy and the angular distribution are in qualitative agreement with the experimental results of ref. [2]. In order to have further comparisons with the experimental data, we have estimated the average neutron multiplicities per primary reaction and kinetic energy carried away by the neutrons (MeV). This is shown in table 1 along with the experimental data [2]. The table also shows the calculated values using the codes TIERCE-Cugnon (INCL) and LAHET-BPQ (BPQ) as given in table V of ref. [2]. In calculating the multiplicity we have divided the differential neutron emission cross-section by the total reaction cross-section σ_{R}. In our calculations we have taken σ_{R} to be the simple geometrical cross-section which is slightly smaller (1539.4 mb) than the reported [2] cross section of 1723 mb for 800 MeV protons on ^{208}Pb. In the 0–2 MeV range, the QMD results for neutron multiplicity (M) and the kinetic energy carried away by the emitted neutrons ($E \times M$) are slightly lower than those calculated with other codes. There is no experimental data available in this energy range. In the 2–20 MeV energy range the QMD results for (M) and ($E \times M$) are

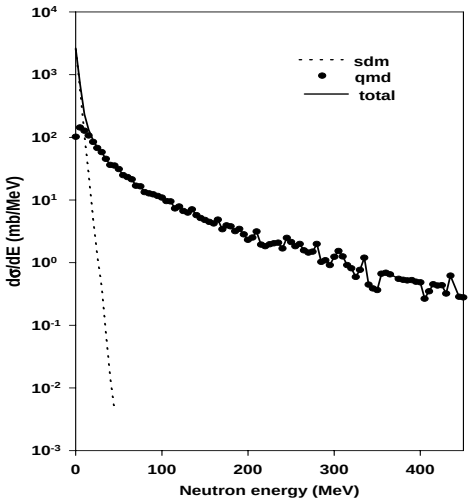

Figure 1. Neutron energy spectra from 800 MeV proton-induced reaction on ^{208}Pb.

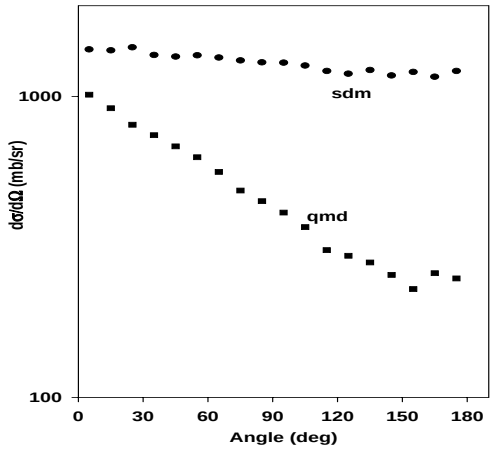

Figure 2. Energy integrated neutron angular distribution from 800 MeV proton-induced reaction on ^{208}Pb.

slightly higher than the experimental as well as the calculated results of the other codes. For 20–$E_{\rm inc}$ energy range, M is very slightly higher than the experimental, INCL and BPQ results. However, ($E \times M$) for QMD is lower than the experimental (though within error bar) and the other two codes. This indicates that the QMD results slightly underpredicts the low energy (less than 20 MeV) neutron production and slightly overpredicts the neutron emissions that are higher than 20 MeV but not of very high energy.

Next we have plotted the multiplicity differential neutron emission cross section $\mathrm{d}\sigma/\mathrm{d}m$ (mb/m) in figure 3 along with the experimental data [1] for 800 MeV protons on 2 mm thick Pb target. For 800 MeV protons this target thickness is considered to be very small

Table 1. Average neutron multiplicity and kinetic energy carried out (800 MeV p on Pb). $M^{\rm QMD}$: multiplicity (QMD), $M^{\rm exp}$: multiplicity (experimental, [2]), $M^{\rm INCL}$: multiplicity (TIERCE-Cugnon), $M^{\rm BPQ}$: multiplicity (BPQ), E: neutron energy in MeV.

	Emission energy (MeV)		
	0–2	2–20	20–$E_{\rm inc}$
$M^{\rm QMD}$	4.48	7.59	2.26
$M^{\rm exp}$		6.5$\pm$0.7	1.9$\pm$0.2
$M^{\rm INCL}$	4.9	6.9	2.2
$M^{\rm BPQ}$	5.2	7.1	2.1
$E \times M^{\rm QMD}$	4.65	46.17	187.57
$E \times M^{\rm exp}$		38$\pm$4	200$\pm$20
$E \times M^{\rm INCL}$	5	42	211
$E \times M^{\rm BPQ}$	5	42	224

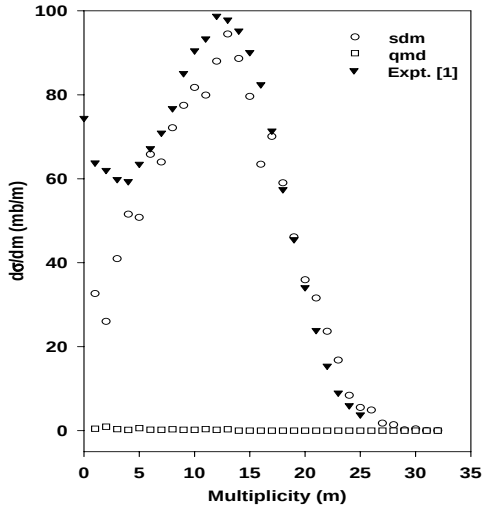

Figure 3. Multiplicity distribution of neutron emission cross-section from 800 MeV proton-induced reaction on ^{208}Pb.

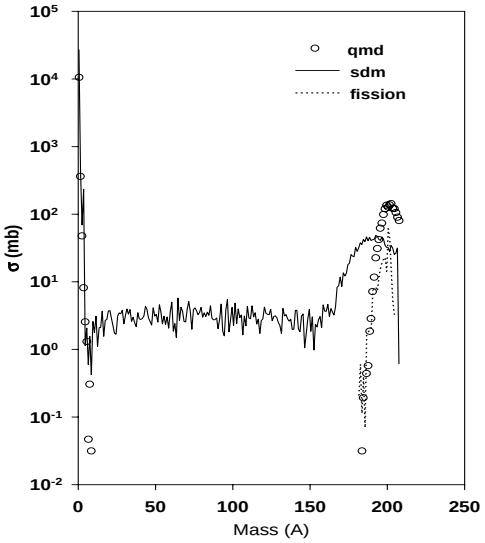

Figure 4. Production cross-section of different mass fragments in 800 MeV proton-induced reaction on ^{208}Pb.

and thus the comparison is justified. The calculated results show SDM and QMD contributions separately with the latter being only a negligibly small portion of the total neutron multiplicity. The QMD+SDM calculations match well in the dominant bell-shaped region of the neutron multiplicities distribution. The most probable multiplicity is around 12–13

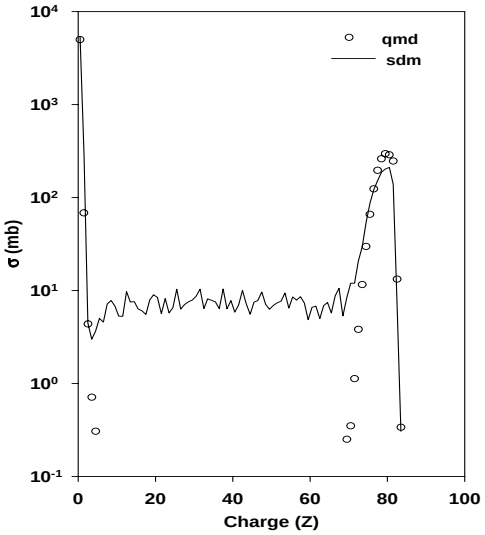

Figure 5. Charge distribution of different spallation products from 800 MeV proton-induced reaction on ^{208}Pb.

in both the cases. However, for very low multiplicities the experimental results exhibit an increasing trend with decreasing multiplicity, which is absent in the present calculated results. It is stated that this part is contributed by weakly inelastic peripheral collisions. This discrepancy needs further investigation since this neutron multiplicity data is important for the design of ADS.

Besides neutron production, formation of fragments in different mass ranges are also important because various radioactive and chemically toxic elements are produced in spallation reactions. A good agreement between QMD calculations and experimental data for neutron production prompted us to estimate the yield distributions of various fragment nuclei in the spallation process. Figure 4 gives the mass (A) distribution of spallation products from QMD, SDM and fission processes. It is observed that dominant productions are of target-like and projectile-like mass fragments with relatively much higher production of the projectile-like fragments (neutrons are the highest). Only the evaporation process is responsible for the production of intermediate mass nuclides. The QMD process contributes only by producing target-like and projectile-like masses. The fission process yields a mass distribution that is confined near the target mass region. The charge (Z) distribution of the product nuclei is plotted in figure 5 separately for the QMD and SDM component. This distribution also shows similar features as that of the mass distribution. Production cross-sections of several important long-lived radionuclides are listed in table 2 along with their half-lives. A knowledge of the yield of these radionuclides are required for radiological safety in accessing the target and nearby areas during maintenance. Table 3 gives the production cross-section of several gaseous elements. The toxic gases cause structural damage to the target material and the beam window.

Table 2. Half-lives and production cross-sections (mb) of some radionuclides produced in 800 MeV proton-induced reaction on ^{208}Pb.

Nuclide	Half-life	Production cross-section (mb)	Nuclide	Half-life	Production cross-section (mb)
^{203}Bi	51.87 h	9.09	^{189}Ir	13.2 d	3.15
^{201}Pb	9.33 h	10.1	^{188}Ir	41.5 h	4.26
^{200}Pb	21.5 h	9.96	^{188m}Ir	4.2 ms	
^{204}Tl	3.78 y	10.36	^{187}Ir	10.5 h	6.12
^{202}Tl	12.23 d	10.9	^{187m}Ir	30.3 ms	
^{201}Tl	72.91 h	11.92	^{186}Ir	16.64 h	5.96
^{200}Tl	26.0 h	10.15	^{186m}Ir	2.0 h	
^{203}Hg	46.61 d	5.86	^{185}Ir	14.4 h	4.83
^{197}Hg	64.14 h	10.03	^{184}Ir	3.09 h	7.54
^{197m}Hg	23.8 h		^{189}Os		5.16
^{195}Hg	9.9 h	11.12	^{189m}Os	5.8 h	
^{195m}Hg	41.6 h		^{185}Os	93.6 d	3.50
^{194}Hg	520 y	10.48	^{183}Os	13.0 h	3.16
^{193}Hg	3.8 h	13.63	^{183m}Os	9.9 h	
^{193m}Hg	11.8 h		^{182}Os	22.1 h	3.89
^{192}Hg	4.85 h	13.23	^{182}Re	64.0 h	2.86
^{200}Au	48.4 m	4.40	^{182m}Re	12.7 h	
^{200m}Au	18.75 h		^{181}Re	19.9 h	3.46
^{198}Au	2.69 d	7.10	^{97}Tc	2.6×10^{6} y	2.07
^{198m}Au	2.27 d		^{97m}Tc	90.1 d	
^{196}Au	6.183 d	6.15	^{96}Tc	4.28 d	1.78
^{196m}Au	8.1 s, 9.7 d		^{96m}Tc	51.5 m	
^{195}Au	186.1 d	6.48	^{80}Br	17.68 m	1.86
^{195m}Au	30.5 s		^{80m}Br	4.42 h	
^{194}Au	38.02 h	8.22	^{77}Br	57.04 h	1.19
^{194m}Au	600 ms, 420 ms		^{77m}Br	4.28 m	
^{193}Au	17.65 h	8.85	^{65}Ni	2.52 h	2.185
^{193m}Au	3.9 s		^{60}Co	1925.1 d	1.56
^{192}Au	4.94 h	8.33	^{47}Sc	3.35 d	1.865
^{192m}Au	160 ms		^{46}Sc	83.79 d	1.841
^{191}Au	3.18 h	10.53	^{46m}Sc	18.75 s	
^{191m}Au	0.92 s		^{45}Ca	162.61 d	2.11
^{195}Pt	33.8%	4.43	^{42}K	12.36 h	1.838
^{195m}Pt	4.02 d		^{32}Si	172 y	2.25
^{193}Pt	50 y	5.13	^{24}Na	24.96 h	1.22
^{193m}Pt	4.33 d		^{24m}Na	20.20 ms	
^{191}Pt	2.96 d	5.07	^{18}F	109.77 m	1.24
^{189}Pt	10.87 h	7.01	^{3}H	12.33 y	50.91
^{192}Ir	73.83 d	3.04			
^{192m}Ir	1.45 m, 241 y				

Table 3. Production cross-section of some gaseous elements from 800 MeV proton-induced reaction on ^{208}Pb.

Element	Production cross-section (mb)
Xe	9.142
Kr	7.53
Ar	5.52
Cl	6.03

4. Conclusion

The QMD calculations alongwith SDM give satisfactory estimates of spallation products. However, further studies at higher incident energies and about the parameters of the code are needed to remove the slight discrepancies observed in the energy distribution of neutron multiplicity and kinetic energy carried away by the emitted neutrons. Based on the observation of an overall good agreement between the experimental data and QMD results we have provided calculated data on the production of gaseous elements and radionuclides that are reasonably long-lived and have significant production cross sections.

References

[1] A Letourneau *et al*, *Nucl. Instrum. Methods* **B70**, 299 (2000)
[2] S Leray *et al*, *Phys. Rev.* **C65**, 044621(1-17) (2002)
[3] K Niita, S Chiba, T Maruyama, T Maruyama, H Takada, T Fukahori, Y Nakahara and A Iwamoto, *Phys. Rev.* **C52**, 2620 (1995)
K Niita, T Maruyama, T Maruyama and A Iwamoto, *Prog. Theor. Phys.* **98**, 87 (1997)
[4] H W Bertini, *Phys. Rev.* **131**, 1801 (1963)
[5] J Cugnon, *Nucl. Phys.* **A462**, 751 (1987)
J Cugnon, C Volant and S Vuillier, *Nucl. Phys.* **A620**, 475 (1997)
[6] L Dressner, Oak Ridge report ORNL-TM-196 (1962)
[7] F Atchison, *Proceedings of a Specialists' Meeting*, OECD/NEA (Issy-le-Moulineaux, France, 1994) p.199
[8] M Blann *et al*, International Code Comparison for Intermediate Energy Nuclear Data, OECD/NEA (1994)
[9] X Ledoux *et al*, *Phys. Rev. Lett.* **82**, 4412 (1999)
[10] M Enke *et al*, *Nucl. Phys.* **A657**, 317 (1999)